Msx1 is expressed in retina endothelial cells at artery branching sites

Miguel Lopes*,‡, Olivier Goupille*,§, Cécile Saint Cloment and Benoît Robert¶

Institut Pasteur, Génétique moléculaire de la Morphogenèse & CNRS URA 2578, 25 Rue du Docteur Roux, 75015 Paris, France

*These authors contributed equally to this work
‡Present address: IPSEN Innovation, Scientific affairs department, 5 Avenue du Canada, 91966 Les Ulis Cedex, France
§Present address: CEA, DSV/IMETI/STI/LEPDS & INSERM U962, 18 Route du Panorama, 92265 Fontenay aux Roses Cedex, France
¶Author for correspondence (benoit.robert@pasteur.fr)

Summary

Msx1 and **Msx2** encode homeodomain transcription factors that play a role in several embryonic developmental processes. Previously, we have shown that in the adult mouse, $Msx1^{lacZ}$ is expressed in vascular smooth muscle cells (VSMCs) and pericytes, and that $Msx2^{lacZ}$ is also expressed in VSMCs as well as in a few endothelial cells (ECs). The mouse retina and choroid are two highly vascularized tissues. Vessel alterations in the retina are associated with several human diseases and the retina has been intensely used for angiogenesis studies, whereas the choroid has been much less investigated. Using the $Msx1^{lacZ}$ and $Msx2^{lacZ}$ reporter alleles, we observed that **Msx2** is not expressed in the eye vascular tree in contrast to **Msx1**, for which we establish the spatial and temporal expression pattern in these tissues. In the retina, expression of **Msx1** takes place from P3, and by P10, it becomes confined to a subpopulation of ECs at branching points of superficial arterioles. These branching sites are characterized by a subpopulation of mural cells that also show specific expression programs. Specific Msx gene inactivation in the endothelium, using **Msx1** and **Msx2** conditional mutant alleles

together with a *Tie2-Cre* transgene, did not lead to conspicuous structural defects in the retinal vascular network. Expression of **Msx1** at branching sites might therefore be linked to vessel physiology. The retinal blood flow is autonomously regulated and perfusion of capillaries has been proposed to depend on arteriolar precapillary structures that might be the sites for **Msx1** expression. On the other hand, branching sites are subject to shear stress that might induce **Msx1** expression. In the choroid vascular layer $Msx1^{lacZ}$ is expressed more broadly and dynamically. At birth $Msx1^{lacZ}$ expression takes place in the endothelium but at P21 its expression has shifted towards the mural layer. We discuss the possible functions of **Msx1** in the eye vasculature.

Introduction

Angiogenesis is the process by which pre-existent vessels rearrange in order to give rise to new vascular beds (Jain, 2003). The mouse retina is one of the best characterized models for *in vivo* vessel formation as it displays all of the morphological hallmarks of angiogenesis (i.e. sprouting, branching, fusion, remodelling and maturation) after birth (Fruttiger, 2002, 2007). In contrast to human, murine newborns do not possess a developed retinal vascular plexus (Gyllensten and Hellstrom, 1954). In these, the superficial retinal vascular plexus forms during the first week after birth by radial outgrowth of vessels from the optic nerve entry point to the periphery (Fruttiger, 2007; Stahl et al., 2010). These superficial vessels reach the retinal edges at approximately post-natal day (P) 9 and from this stage onwards, vertical sprouting forms the deep and then intermediate vascular beds, that reach the retinal periphery at approximately P12 and P15, respectively. The three retina vascular beds become fully mature and interconnected at the end of the third postnatal week (Stahl et al., 2010). At this stage, the retinal superficial vasculature is composed of six major arteries and veins that form primary branches into arterioles and venules. Arterioles and

venules branch into a capillary network that is in direct contact with deep and intermediate layers. This network is covered with pericytes, providing retina with the densest coverage of pericytes in the whole vasculature (Shepro and Morel, 1993). The choroidal vascular system, which resides between the retina and the sclera, is fully developed before birth and supplies oxygen and nutrients to the avascular retina (Campochiaro, 2000). At early stages, the blood supply of the eye is also provided by the hyaloid vasculature that originates from the central hyaloid artery in the optic nerve and extends through the primitive vitreous toward the anterior segment (Saint-Geniez and D'Amore, 2004). The hyaloid vasculature regresses when ocular development proceeds in order to leave a transparent visual axis (Mitchell and Gingras, 1998; Brown et al., 2005).

Blood vessels are mainly composed of an inner endothelial cell (EC) layer externally covered by mural cells, namely vascular smooth muscle cells (VSMCs) in arteries and veins, and pericytes in capillaries (Jain, 2003). In the mature vascular plexus, mural cells contribute to endothelial tube stabilization, maintenance of vascular permeability and regulation of the blood flow. In small arterioles and capillaries, most of these activities are performed

by pericytes (Orlidge and D'Amore, 1987; Sato and Rifkin, 1989; Diaz-Flores et al., 2009; Armulik et al., 2011). In the central nervous system, not all the pericytes contain the muscle-specific actin isoform, only those in the pre- and postcapillary regions (i.e. on arterioles and venules) (Nehls and Drenckhahn, 1991; Rucker et al., 2000). This led to the proposition that blood flow is regulated mainly at the level of precapillary arterioles (Anderson and McIntosh, 1967; Baez, 1977). However, time-lapse and functional analyses have demonstrated that capillaries are capable of regulating blood flow along their whole length (Metea and Newman, 2006; Peppiatt et al., 2006). In the eye, vasoconstriction and vasodilatation via the pericytes are evoked by light-induced stimulation of perivascular astrocytes (Metea and Newman, 2006).

Msx genes encode homeodomain transcription factors and are essential for normal craniofacial and limb development, nervous system patterning, eye formation, as assessed by phenotypic abnormalities in knock-out mice (Bach et al., 2003; Wu et al., 2003; Ishii et al., 2005; Lallemand et al., 2005, 2009). In the cardiovascular system, Msx genes have previously been shown to be important for outflow tract patterning (Ishii et al., 2005; Chen et al., 2007), head vessel maturation (Lopes et al., 2011) and adult vessel calcification (Towler et al., 2006). In adult mice, $Msx2^{lacZ}$ is mainly expressed in a subset of VSMCs in peripheral arteries and veins (brachial, femoral and caudal), as well as a few ECs of the aorta. $Mxs1^{lacZ}$ is expressed to a lesser extent by VSMCs of peripheral arterial trunks, but is highly expressed in mural cells of arterioles and capillaries that irrigate the tissues (Goupille et al., 2008).

In this paper, we observe that $Msx2^{lacZ}$ expression is not detectable in eye vessels, and describe *Msx1* expression patterns in the retina and choroid vasculature. In the choroid, $Msx1^{lacZ}$ is expressed in a broad dynamic pattern, initially in the endothelium. Expression is observed later on in VSMCs, similar to *Msx1* general behaviour in the peripheral vasculature. In contrast, in the retina, $Msx1^{lacZ}$ expression is restricted to ECs of the arteriolar branching points in the superficial vascular network. At these branch points, we further characterised a sub-population of pericytes, which express high levels of NG2, α-SMA and desmin. We thus demonstrate specific properties of cells constituting these branching structures, not only in the mural layer but also in the endothelial layer.

Results
Kinetics of *Msx1*^{lacZ} expression in vessels of the developing retina
Outgrowth of vessels in the retina occurs postnatally from the central optical disc. This results in the formation of a stereotyped vascular network (Fruttiger, 2007). Analysis of $Msx1^{lacZ}$ mice at P0 revealed that the primitive plexus was formed of ECs and did neither express smooth muscle actin, nor *Msx1* (Fig. 1A,A′, arrowheads). The hyaloid vasculature, which is present during prenatal development and regresses shortly after birth, expressed strong levels of $Msx1^{lacZ}$ as revealed by Xgal staining, and was covered with α-SMA-expressing mural cells (Fig. 1A,A′, arrows). Considering the morphology of the β-galactosidase (β-gal)-positive nuclei and their position relative to isolectin B4 (Ib4) and α-SMA domains, *Msx1*-expressing cells were likely ECs. At P3, retinal arteries have started to form from the primitive plexus. These arteries, which were part of the newly-formed vascular plexus (Fig. 1B′; data not shown), were covered

with α-SMA-positive mural cells. In these arteries, *Msx1* expression was detected in cells with elongated nuclei, suggesting they belonged to the endothelium (Fig. 1B,B′, arrows). At this stage, no *Msx1* expression could be detected in less mature vessels not covered by mural cells (Fig. 1B,B′, arrowheads). At P10, the superficial vessels have reached the peripheral edge of the retina, the capillary bed has begun to develop into the deeper layers and circulation has started (Brown et al., 2005; Fruttiger, 2007). Strikingly, at this stage $Msx1^{lacZ}$ expression became restricted to primary branching points in arterioles (Fig. 1C,C′, arrows). Restricted expression was not yet completed by P12, since a few cells were still expressing *Msx1* along the length of arteries (Fig. 2A, arrowheads), but was achieved at P14 (Fig. 1D,D′). In most cases, more than one nucleus was labelled (Fig. 1F, Fig. 3D-F, Fig. 4A,C). At the branching points, we further observed strong Ib4 concentration that co-localized with *Msx1*-expressing cells (Fig. 1C′-F′, arrows). Ib4 is known to bind the basement membranes (specifically, the versican protein) and thus can label not only ECs but also microglial cells and probably other cell types including some vascular mural cells. On trypsin-digested retinas, Ib4 was unambiguously associated with vessels (not shown). Maximum *Msx1* expression occurred between P14 and P23 (Fig. 1D–E), but expression was maintained at high levels up to P480 (Fig. 1F) and probably lasts over the lifetime of the animal. From P14, we observed that *Msx1* also labelled secondary branches in the arteriolar network (Fig. 1F, Fig. 4D). Noticeably, at all stages, *Msx1* expression was observed only in rather mature arteries that were covered by a SMA-positive mural cell coating suggesting that *Msx1* expression in the endothelium requires EC-VSMC interactions. *Msx1*-labelled branching sites were quantitated throughout development (Fig. 2). There was a large and steady increase between P9 and P23 and thereafter the number plateaued. Therefore, restriction of the expression to branching sites lagged behind the formation of the vascular superficial bed, for which arteries reach the retinal periphery around P8 (Fruttiger, 2007). This was not achieved before the onset of blood flow, which in the mouse retina takes place between P3 and P4 (Brown et al., 2005). From P23, we observed *Msx1* expression at all primary, and some secondary, branching points along the main retinal arteries.

Arteries and veins were identified in flat mounts by virtue of their distinct morphologies and differential coating by mural cells. We did not observe $Msx1^{lacZ}$ labelling of venules in the retina (data not shown), as in any other veins (Goupille et al., 2008). Only the superficial vascular network was labelled. This is in keeping with the fact that deeper beds are primarily formed by sprouting from veins (Fruttiger, 2007). Xgal staining reflected the specific expression of *Msx1* in retinal vessels since no staining was observed in normal mice (data not shown). In contrast to what was observed in peripheral arteries (Goupille et al., 2008), $Msx2^{lacZ}$ could not be detected in hyaloid, retina or choroid vessels at any stage of their development (data not shown).

Msx1^{lacZ} is expressed specifically in ECs
Xgal staining is useful for a broad analysis of expression patterns. However, it does not provide sufficiently high resolution for precise co-localization studies using optical microscopy. In order to identify in which cell type $Msx1^{lacZ}$ is expressed, we used an anti β-gal antibody together with endothelial-specific (anti-CD31) and mural-specific (anti-α-SMA) antibodies, to perform
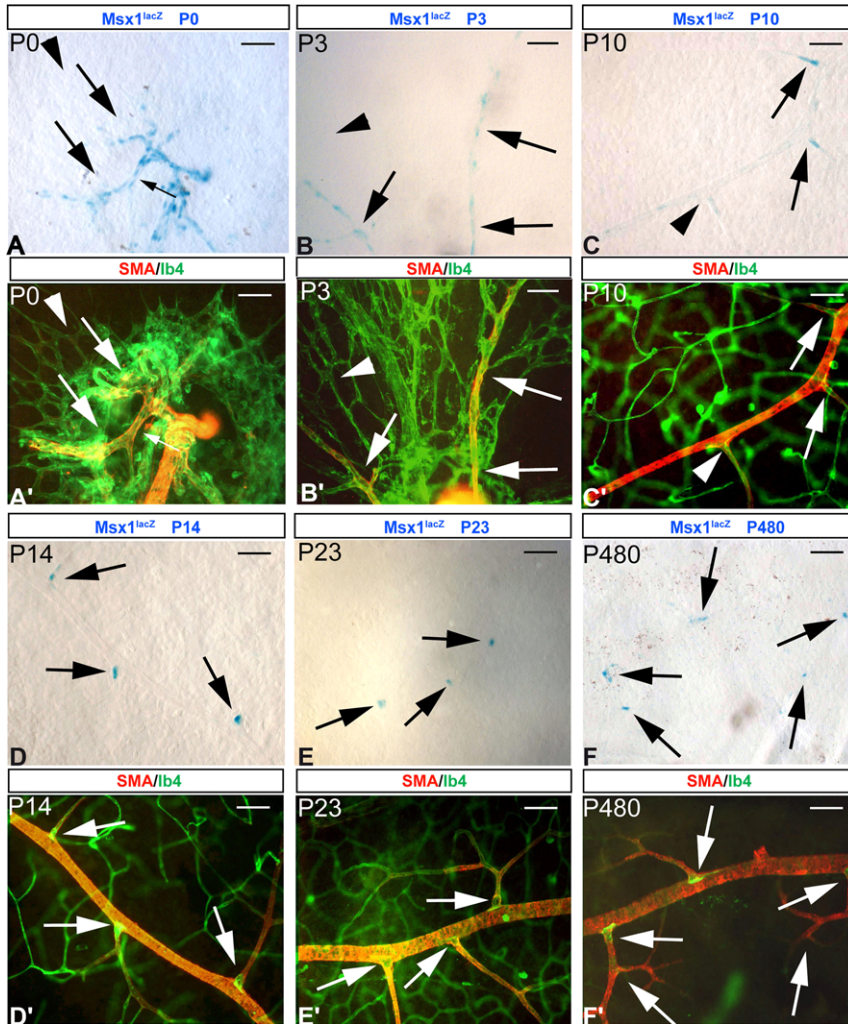
Fig. 1. Kinetics of *Msx1^{lacZ}* expression in the retina.
Flat-mount retinas from P0, P3, P10, P14, P23 and P480 *Msx1^{nlacZ+/−}* mice were analysed. (A–F) show light microscopy views in which Xgal staining (blue, arrows) labels the nucleus of *Msx1*-expressing cells. (A′–F′) show the corresponding fluorescence fields for ECs (IB4, green) and mural cells (α-SMA, red). At P0 (A, A′), the superficial plexus that is just beginning to develop around the optic nerve does not express *Msx1^{lacZ}* (arrowheads). At the same stage the hyaloid vessels are covered with α-SMA-positive cells and are labelled with Xgal (arrows). At P3 (B, B′), *Msx1^{lacZ}* is expressed in elongated nuclei along the first formed retinal arteries (arrows) that are covered with α-SMA-positive cells. Note that these arteries are in continuity with the vascular immature, endothelial plexus that does not express *Msx1^{lacZ}* (arrowheads). Around P10 (C, C′), Xgal staining starts to concentrate at the primary branching sites of the superficial retinal arteries (arrows). Note that some branching sites express *Msx1* very weakly at this stage (arrowheads). Expression is observed in all primary branch points at later stages, such as P23 (E, E′) and P480 (F, F′), and even at some secondary branches (F, F′). Xgal staining was most intense between P14 and P23 (D, E). In all panels, scale bar =50 μm.
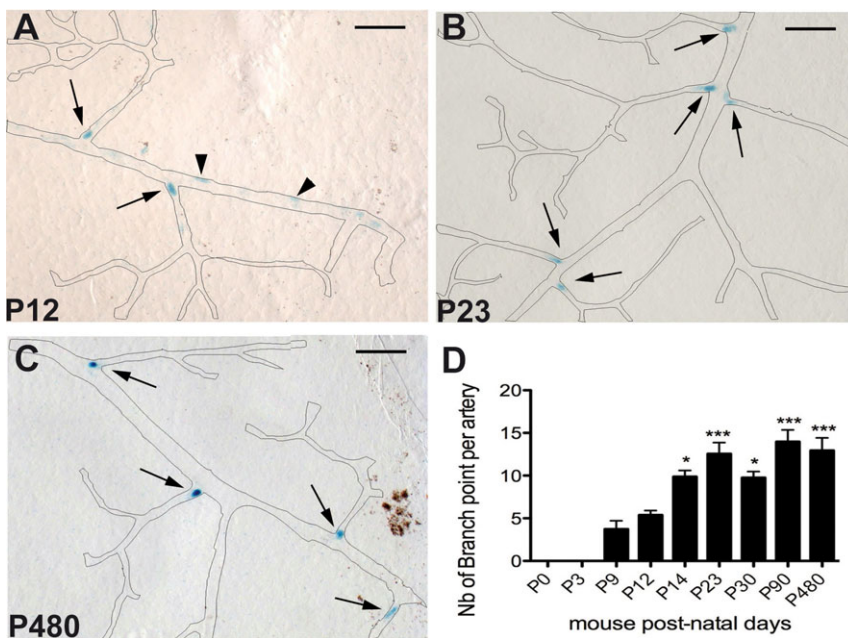

Fig. 2. Quantification of *Msx1*-expressing branching sites during retinal vessel development. At P12 (A), some expression is still observed along the vessels (arrowheads) in addition to branch sites (arrows). From P23 to P480 (B,C), expression is restricted to branch sites (arrows). In A–C, artery layout is depicted for legibility. (D) shows the total number of branch points along a single main artery that express *Msx1* at each stage analysed. At P0 and P3, no *Msx1*-positive branching points were observed. They then increased significantly in number from P9 to P23. From this stage, this number remained stable. n=6, (*) $P<0.05$, (**) $P<0.01$, (***) $P<0.001$. In panels A–C, scale bar =50 μm.
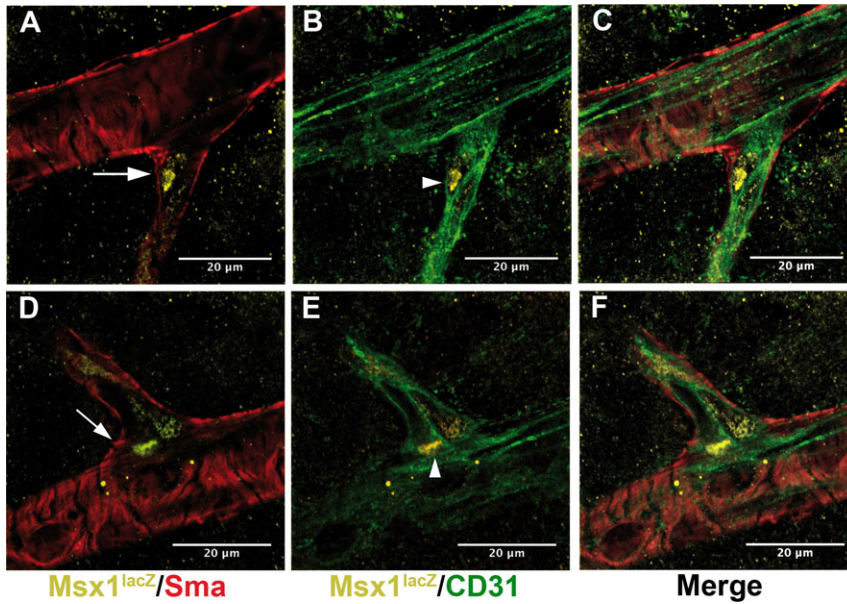
Biology Open

Fig. 3. *Msx1^lacZ* is expressed specifically in the endothelial layer. Confocal images of flat mount retinas from P21 mice, stained for (A,C,D,F) mural (α-SMA, red) or (B–F) endothelial (CD31, green) markers and β-gal (A–F, yellow). At branching sites, the β-gal signal is nuclear and is completely restricted to CD31-positive cells (B,E, arrowheads), which are themselves ensheathed in the α-SMA-positive cell layer (A,D, arrows). This is particularly obvious in merged images (C,F), demonstrating that β-gal-expressing cells are endothelial cells. In all panels, scale bar =20 μm.

Msx1^lacZ/Sma   Msx1^lacZ/CD31   Merge

confocal microscopy on flat mount retinas. This showed that the *Msx1* reporter gene is expressed in ECs (Fig. 3B,E, arrowheads) and not in mural cells (Fig. 3A,D, arrows). Indeed, the nuclear β-gal signal was completely surrounded by CD31 protein and was observed in a luminal position relative to the mural marker α-SMA (Fig. 3C,F). As expected, β-gal colocalized with nuclear Hoechst staining, since the *lacZ* gene in this transgenic mouse is associated with a nuclear localisation sequence (not shown).

Correlation between expression of *Msx1* and branch point-characteristic proteins

To get insight into the role of *Msx1* at arteriolar branching points, we investigated possible correlations with accumulation of other proteins. We co-stained the retina from *Msx1^lacZ* animals for β-gal together with α-SMA (Fig. 4A,A′), desmin (Fig. 4B,B′) and NG2 (Fig. 4C,C′). In the rat retina, NG2 and desmin are expressed in immature mural cells around birth, but NG2 is expressed in pericytes in the adult and weakly in arteriole and vein VSMCs, whereas desmin remains at a high level in pericytes and VSMCs. On the contrary, α-SMA, which is also expressed in immature mural cells, becomes highly expressed in VSMCs and weakly in pericytes after birth (Hughes and Chan-Ling, 2004). According to our data, the primary branching structures were supported by a sub-population of mural cells that expressed α-SMA (Fig. 4A′), desmin (Fig. 4B′) and NG2 (Fig. 4C′). Of note, calponin is expressed primarily in VSMCs, although it has been described in pericytes of aged animals (Hughes and Chan-Ling, 2004; Hughes et al., 2006). Calponin was expressed in a fraction of branching structures, and always in cells on the distal side relative to the arteriole (not shown). Thus, at the branch sites, the sub-population of mural cells differs from others by its capacity to express simultaneously VSMC-associated proteins, such as α-SMA and calponin, together with pericyte markers like NG2 and desmin. Of note, α-SMA, desmin and calponin are proteins that participate in contraction, making this structure a candidate for specific contractile properties. Furthermore, according to Ib4 (Fig. 1C′–F′) and laminin (Fig. 4D′, arrows) expression levels, the density of the basement membrane at these branching points appeared high.

No apparent developmental defect in *Msx1* ^flox/ flox *Msx2* ^flox/ flox Tie2Cre mutant

To further investigate the possible function of Msx genes in the retinal endothelium, we inactivated *Msx1* and *Msx2* specifically in ECs, taking advantage of the previously described *Msx1^flox* (Fu et al., 2007) and *Msx2^flox* (Bensoussan et al., 2008) alleles, and the *Tie2-Cre* transgene (Kisanuki et al., 2001). Only *Msx1* is expressed in the retina; however *Msx2* was also inactivated to avoid any compensation between the two genes (Ishii et al., 2005; Lopes et al., 2011).

Tie2-Cre has been shown to specifically induce loxP site recombination in the retina EC plexus (Ye et al., 2009; Weskamp et al., 2010; Sweet et al., 2011). However, no data has been reported referring to the efficiency of this transgene in ECs at branching site. To ascertain this point, we associated the Rosa^mT/mG reporter gene (Muzumdar et al., 2007), that expresses *Tomato* red before and *Gfp* after loxP recombination, with the *Tie2-Cre* transgene. GFP was revealed on dissected retinas using specific anti-GFP antibodies, together with antibodies against endothelial (CD31) or mural (α-SMA) markers. This demonstrated recombination in all ECs, including those residing at branching sites (supplementary material Fig. S1).

These data allowed us to perform the functional analysis. Dissected retinas from *Msx1* ^flox/+ *Msx2* ^flox/+ Tie2-Cre and *Msx1* ^flox/ flox *Msx2* ^flox/ flox Tie2-Cre mice were labelled for CD31, α-SMA and desmin, then analysed in flat mount by confocal microscopy. *Msx1* and *Msx2* inactivation in the endothelium did not result in major structural defects, neither at P7, when the vessels are intensely sprouting (Fig. 5A-F), nor in two months-old animals, when angiogenesis is achieved (Fig. 5G–L). At the two stages, CD31 staining (Fig. 5A,D, C,F and G–J) did not reveal either over- or under-branching in arteries, where *Msx1^lacZ* is expressed. Furthermore, considering the intensity of α-SMA (Fig. 5B,E and H,K) and desmin (Fig. 5I,L) signals, there was no conspicuous reduction in VSMC coverage or decrease in the expression of contractile proteins at branching sites. In the retina, desmin is strongly expressed in pericytes (Hughes and Chan-Ling, 2004), and we could not detect any difference in the number of desmin-positive cells in capillaries of mutant versus control embryos (Fig. 5I,L).
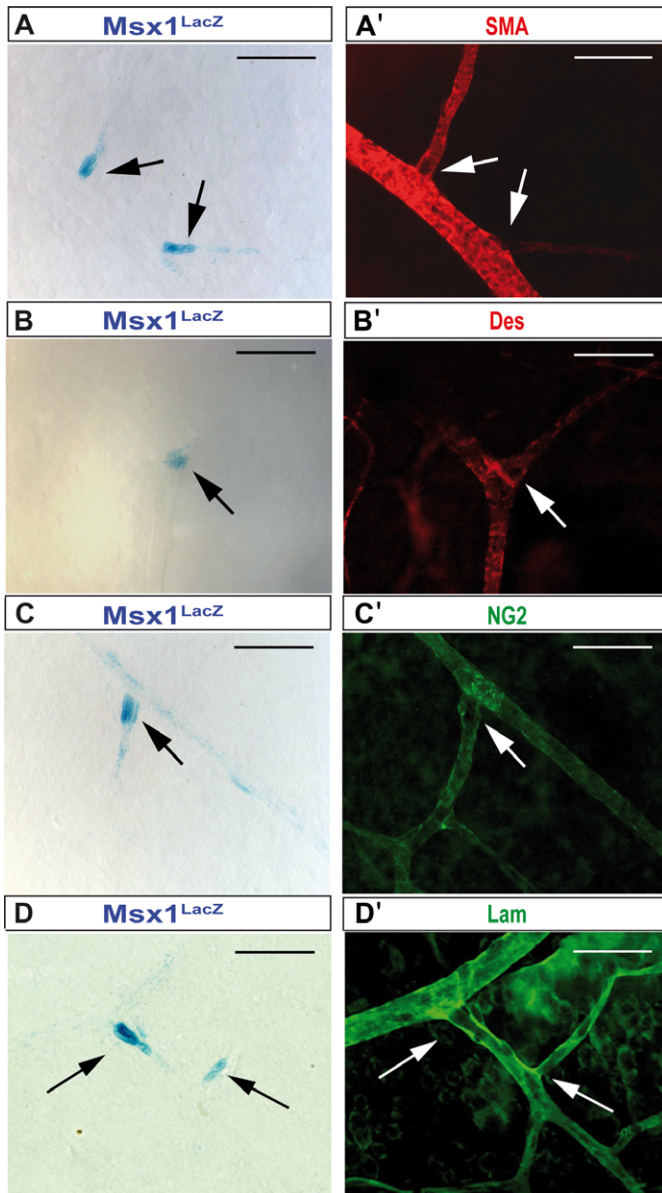
Fig. 4. Characterization of the *Msx1*-expressing branching points. Flat-mount retinas from P14 *Msx1*^{lacZ} mice were stained with Xgal (A–D) in combination with antibodies against α-SMA (A′, red), desmin (B′, red), the pericyte marker NG2 (C′, green), or the basal lamina protein laminin (D′, green). α-SMA labels VSMCs and a population of pericytes that are concentrated at the beginning of the primary branches (A,A′, arrows). Most of the mural cells observed at the major branching points also express desmin (B′) and NG2 (C′). Laminin signal is strongest in the major arterioles and at the beginning on the primary branches (D′). The vast majority of primary, and some secondary, branches do express *Msx1*^{lacZ} (D,D′). *Msx1*^{lacZ}-positive cells adopt a luminal localization relatively to the mural markers. In all panels, scale bar =50 μm.

Msx1 is broadly expressed in choroid vessels

To verify whether this branch site-restricted expression pattern is more widespread in the eye vasculature, we investigated *Msx1* expression in the choroid. In the mouse, choroidal vasculature is fully developed before birth and supplies oxygen and nutrients to the anterior region of the retina (Campochiaro, 2000). Similar to the retinal vasculature, it develops according to a stereotyped pattern, constituted of major arteries that grow from the optic

nerve entry point toward the periphery. *Msx1*^{lacZ} expression was detectable as early E16.5 and became conspicuous at E17.5. At these stages, expression took place in arterioles covered with α-SMA-expressing mural cells and also in mural cell-free capillaries (data not shown). At P0, *Msx1*^{lacZ} was broadly expressed in choroidal vessels, at a high level (Fig. 6A,A′). On flat mounts, expression was observed in internal, longitudinal cells, which matched Ib4 labelling, suggesting it took place in ECs. Similar to prenatal stages, expression was observed in mural cell-covered (Fig. 6A,A′, arrows) as well as mural cell-free (Fig. 6A,A′, arrowheads) arteries. Surprisingly, at P14 and later, *Msx1*^{lacZ} expression was detected in cells resembling mural cells, since the β-gal-positive nuclei exhibited a rounder shape and a more external position (Fig. 6B,B′). Furthermore, expression was now restricted to mural cells-covered arteries. We analysed *Msx1*^{lacZ} expression until P150 and the location and intensity of Xgal staining did not change with age (Fig. 6C,C′).

To confirm the shift in expression of *Msx1*^{lacZ} from endothelial to mural cells, we performed a confocal analysis of choroid transverse sections. At P0, the nuclear β-gal protein was observed in most CD31-positive cells of the major arterioles (Fig. 7A, arrows). Clearly, α-SMA-positive cells did not accumulate β-gal protein (Fig. 7B, arrowheads). At P21 the localization of β-gal had changed dramatically: CD31-surrounded nuclei appeared completely devoid of β-gal protein (Fig. 7C, arrows) whereas α-SMA-positive cells expressed high levels of this protein (Fig. 7D, arrowheads). This change in pattern was observed in the whole choroid vascular tree as shown in Fig. 6.

Discussion

Studying the different structures that compose the retina and choroid vasculature may give insight into disease processes such as diabetic or hypertensive retinopathy, hypertensive choroidopathy and macular degeneration. Taking advantage of *Msx1*^{lacZ} and *Msx2*^{lacZ} knock-in mice, we have established that *Msx1*, but not *Msx2*, is expressed in the mouse retinal and choroidal vasculature. One of the most striking results we obtained is the specific expression of *Msx1* in a cluster of ECs at primary, and sometimes secondary, arteriolar branching sites in the retina. This property might be more widespread in the peripheral vasculature. We previously reported that *Msx1* expression is more intense in arterioles of the thigh muscle at branching sites (Goupille et al., 2008). Our data suggested that expression took place in VSMCs, but the situation should be revisited using confocal microscopy at these sites. The expression pattern we observe in retina raises questions about the function *Msx1* may play and the mechanisms that might activate it at branching sites.

Msx1 is unlikely to be associated with formation or stabilization of retinal arteriole branches, since disruption of the *Msx1* gene specifically in the endothelium does not lead to defects in branching frequency or branch stability. A function related to vessel physiology is therefore more likely. In any case, *Msx1* may be responding to specific signalling molecules at these sites. The Notch pathway is of particular relevance to this issue. The initial pattern of *Jag1* expression in the retina is different from that of *Msx1*, but at P15, Jag1-positive cells are concentrated at branch points in arteries, in both endothelial and mural cells, in a pattern strikingly similar to *Msx1* (Hofmann and Luisa Iruela-Arispe, 2007). However, *Jag1* null mice die by E11.5 as a result of a lack of vascular remodelling (Xue et al.,
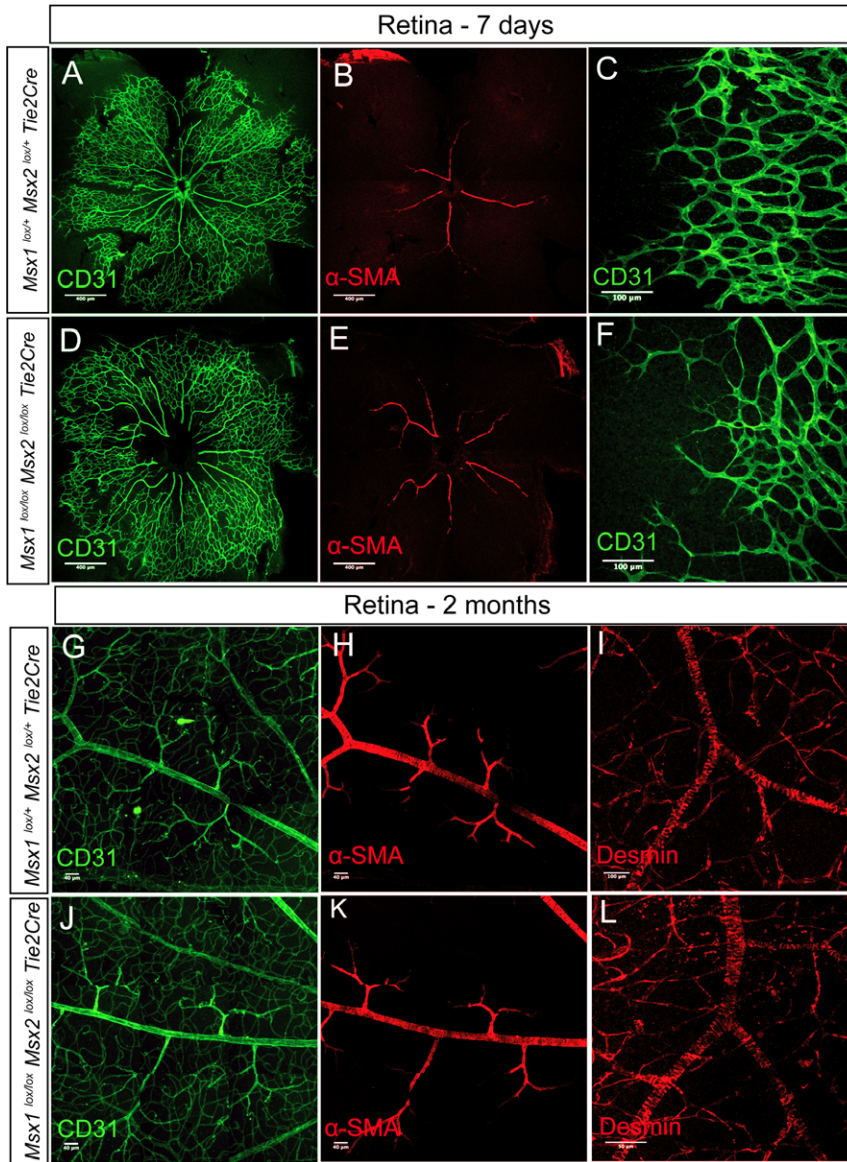
Fig. 5. There is no evident phenotypic alterations in the *Msx1* flox/ flox *Msx2* flox/ flox *Tie2-Cre* mouse retinas. Retinas from heterozygous (A–C) or mutant (D–F) P7 mice were stained for CD31 (green, A,D,C,F), α-SMA (red, B,E); similarly, retinas from 2 months old mice were stained for CD31 (green, G,J), α-SMA (red, H,K) and desmin (red, I,L). At P7, the overall structure of retina vasculature does not look changed (A,D) in mutants. Close up images of the angiogenic front do not show differences in vascular density or in the morphological characteristics and number of tip cells (C,F). At this stage, only the main arterial branches are covered by VSMCs in both the mutant (E) and the control (B). In retinas from 2 month-old mice, the density of branches along the endothelial tube appears unchanged in the mutant according to CD31 staining (G,J). The intensity and number of cells expressing α-SMA is similar between the *Msx1* flox/ flox *Msx2* flox/ flox *Tie2-Cre* mutant (K) and the *Msx1* flox/+ *Msx2* flox/+ *Tie2-Cre* control (H). The desmin-positive population of pericytes does not look affected by the endothelial-specific Msx gene inactivation (I,L). Note that, in D, the centre of the retina was accidentally lost during dissection. In panels A,B and D,E, scale bar is 400 µm, in panels G,H and J,K, 40 µm, in panels C, F and I, 100 µm and in panel L, 50 µm, respectively.

1999), a phenotype very different from the one observed in *Msx1* single or *Msx1*; *Msx2* double null mutant (Satokata et al., 2000; Lallemand et al., 2005). Furthermore, Notch signalling plays a major role in controlling sprouting and at P6, in endothelium-specific *Jag1* mutants, the density of newly formed vessels at the periphery of the retina is clearly reduced (Benedito et al., 2009). This phenotype was not observed in the endothelium-specific mutation of *Msx1* (Fig. 5C,F). Altogether, these considerations imply that, if *Msx1* is involved in the Notch pathway, it relays only a fraction of Notch activity. *Tie1*, an endothelial-specific receptor of the Tie receptor tyrosine kinase family with unknown ligand, is also expressed in the retinal vessels, and further concentrated at branching sites (Porat et al., 2004). Other signalling pathways, not yet characterized in the retinal vasculature, may play a role in *Msx1* expression.

Conspicuously, branching sites in retinal arterioles form specific structures, which have been designated as arteriolar annuli (Henkind and De Oliveira, 1968; Simoens et al., 1992). These are characterized by hypercellularity and specific or

enhanced expression of a number of genes. Among these are α-*Sma*, *Vimentin* (Bandopadhyay et al., 2001) and *Jag1* (Hofmann and Luisa Iruela-Arispe, 2007). Our own data confirm and extend these reports; in particular, they demonstrate that mural cells at the branching sites express *NG2*, the most characteristic marker of pericytes to date (Ozerdem et al., 2001), and simultaneously, α-*Sma* and *calponin*, which, in mature retinal vasculature, are essentially restricted to VSMCs (Hughes and Chan-Ling, 2004). The basement membrane, which is formed by a synergistic process between endothelial and mural cells, is also modified at *Msx1*-expressing bifurcation points. A higher density of basement membrane proteins such as versican (which was detected by Ib4) and laminin is observed. Noticeably, *Msx1* does not seem to play a role in endothelial secretion of basement membrane proteins since Ib4 and laminin staining in *Msx1* flox/ flox *Msx2* flox/ flox *Tie2Cre* retinas is completely normal (data not shown). Altogether, our data show that, in addition to mural cells, ECs at branching sites also exhibit specific expression programs as assessed by *Msx1* expression.
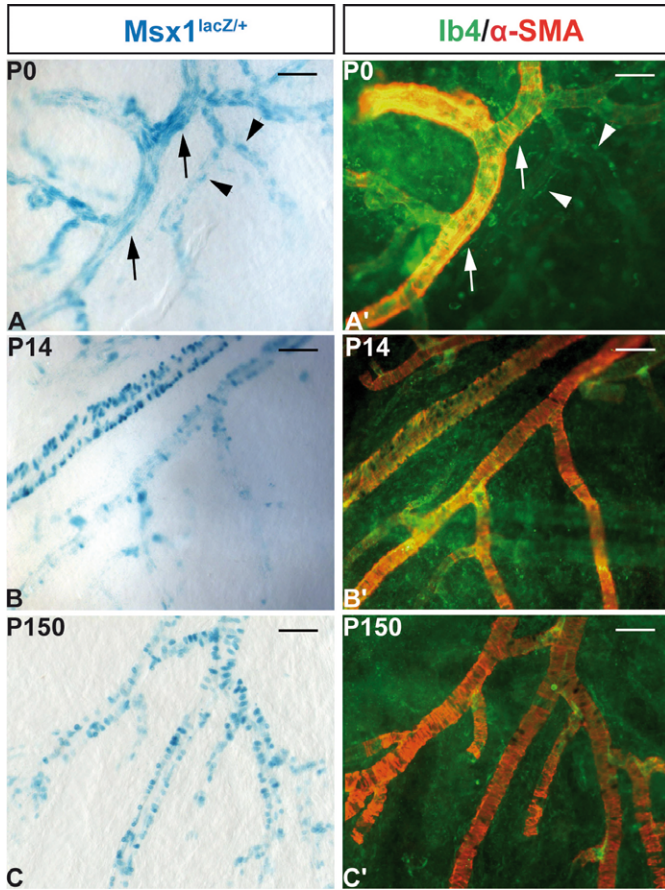
Fig. 6. Kinetics of *Msx1^{lacZ}* expression in the mouse choroid. Flat-mounted choroids at P0, P14 and P150 were stained with Xgal (blue), anti-α-SMA antibody (red) and Ib4 (green), demonstrating a broad expression of *Msx1^{lacZ}* in choroidal vessels. At P0 (A,A′), *Msx1*-expressing cells seem to be in a luminal position relative to α-SMA and to coincide with Ib4 labelling. At this stage, they are observed in vessels either covered with α-SMA-positive cells (arrows) or not (arrowheads). At P14 (B,B′), *Msx1^{lacZ}* expression is still strong in the arterioles and major capillaries, but the β-gal-positive nuclei look rounder and their position appears more to the exterior. At P150 (C,C′), this pattern of expression in maintained. In all panels, scale bar =50 μm.

Fig. 7. Dynamic expression of *Msx1^{lacZ}* in the choroidal vessels. Immunofluorescence was performed on transverse sections of mouse choroids. VSMCs were labelled for α-SMA (red), ECs for CD31 (green) and *Msx1^{lacZ}* expression was revealed using anti-β-gal antibodies (yellow). At P0, the β-gal protein can be observed in CD31-expressing endothelial cells (A, arrows), α-SMA expressing cells are completely negative for β-gal (B, arrowheads). At P21, the endothelial CD31-positive cells do not contain β-gal (C, arrows), in contrast to VSMCs that are strongly labelled for β-gal (D, arrowheads). These results reflect an EC-to-VSMC shift of *Msx1^{lacZ}* expression during the first three weeks after birth. In all panels, scale bar =10 μm.

Hyperaemia (i.e. the increase in blood perfusion associated with neural activity), which is at the basis of functional neuroimaging (Magistretti and Pellerin, 1999), implies mechanisms to regulate blood flow. These have been proposed to take place at the precapillary level in the arteriole (Anderson and McIntosh, 1967). However, the existence of a precapillary sphincter in the retina at the junction between arterioles and capillaries is controversial, has been poorly documented in recent years and the sphincter itself not always rigorously defined (Friedman et al., 1964; Anderson and McIntosh, 1967; Wiedeman et al., 1976; Baez, 1977). From structural analyses, some investigators reported its existence (Benjamin et al., 1998; Ikebe et al., 2001), while other could not detect it (Pannarale et al., 1996). Furthermore, theoretical and experimental studies have shown that regulation of blood flow at the precapillary level is unlikely to play a major role in the capillary filtration coefficient (Bentzer et al., 2001; Boas et al., 2008). Functional analyses indicate that flow regulation takes place over the whole capillary network, via a coupling between astrocytes and blood vessels (Zonta et al., 2003; Cauli et al., 2004; Metea and
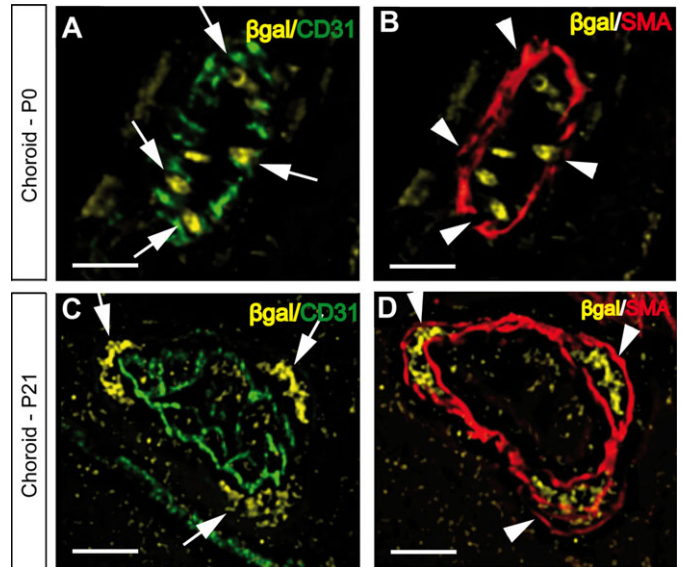
Newman, 2006; Peppiatt et al., 2006). However, a more recent functional study, based on laser speckle flowmetry, suggests that in the retina, activity-dependent changes in blood flow are controlled largely by arterioles and that capillaries contribute little to them, without documenting specific structures responsible for this control (Srienc et al., 2010). *Msx1* expression in the retina is restricted to primary and secondary branching sites between arteries and arterioles. At these sites, contraction-associated proteins are concentrated, and it is plausible that *Msx1* may play a role at the arteriolar level in controlling blood flow.

Arteriolar annuli, and also *Msx1* expression, could be linked to mechanical constraints at branching sites. Vascular bifurcations are associated with local modifications in rate and pattern of blood flow, including low wall and high oscillatory shear stress (Zarins et al., 1983). Noticeably, the ECs are primarily affected by shear stress, as they are in direct contact with blood flow. Indeed, genes in the endothelium are activated in response to shear stress (Andersson et al., 2005; Ni et al., 2010) via specific DNA responsive elements (Boon and Horrevoets, 2009). In addition, increased hemodynamic stresses *in vivo* enhance smooth muscle cell coverage of microvessels (Van Gieson et al., 2003). Shear stress is not negligible in retina arteries and arterioles (Ganesan et al., 2010), thus *Msx1* expression may be linked to blood flow at branching sites. Noticeably, restriction of *Msx1* expression at these sites correlates with the onset of blood flow in the deeper vascular beds of the retina (Stahl et al., 2010), which might substantially change shear stress at bifurcations. It would be necessary to perform arterial obstructive lesions in the retina to evaluate the relation between blood flow and *Msx1* expression.

Another intriguing result that we have obtained concerns the *Msx1^lacZ^* pattern of expression in the choroid, which shifts from endothelial to mural cells in the first three weeks of life (Fig. 7). Previously, we published that *Msx1* is expressed in adult mouse VSMCs and pericytes and, in the embryo, in ECs and VSMCs (Goupille et al., 2008). However, we have never observed expression of *Msx1* in endothelial and mural cell populations in the same vascular bed, either simultaneously or consecutively. Both cells types are regulated by distinct mechanisms and *Msx1* has been associated with a number of different cells types in distinct developmental contexts. Therefore, we think that *Msx1* plays different and independent roles in the endothelial and mural lineages. In addition, we should stress that, after P21, the *Msx1* pattern of expression observed in the choroid is quite similar to the pattern observed in other peripheral arterioles and capillaries (Goupille et al., 2008).

Materials and Methods
Mice
Generation of *Msx1^lacZ^*, *Msx2^lacZ^* and *Msx2^flox^* mutant mice has been described previously (Houzelstein et al., 1997; Lallemand et al., 2005; Bensoussan et al., 2008). The *Msx1^flox^* conditional mutant (Fu et al., 2007) was a generous gift from Dr. Robert Maxson (Los Angeles, California, USA), the *Tie2-Cre* transgenic mouse (Kisanuki et al., 2001), from Dr. Masashi Yanagisawa (Dallas, Texas, USA). The α-*Sm22Cre* (Holtwick et al., 2002) and *Rosa^mT/mG^* reporter mouse (Muzumdar et al., 2007) were purchased from The Jackson Laboratory (Bar Harbor, ME, USA). All strains were maintained on an NMRI outbred background. Genotyping primers were previously described (Lopes et al., 2011). Phenotypic analyses were conducted with mutant embryos using littermates as controls. Animals were housed in the Institut Pasteur animal facilities accredited by the French Ministry of Agriculture to perform experiments on live mice (accreditation # B 75 15-05, issued on May 22, 2008), in appliance of the French and European regulations on care and protection of the Laboratory Animals (EC Directive 86/609, French Law 2001-486 issued on June 6, 2001). Protocols were approved by the veterinary staff of the Institut Pasteur animal facility and were performed in compliance with the NIH Animal Welfare Insurance #A5476-01 issued on 02/07/2007.

Processing of eye tissues
Eyes were collected at postnatal days 0 to 480 (P0-P480). Eyes were enucleated and immediately fixed with 4% paraformaldehyde in phosphate-buffered saline (PBS) pH 7.2 (Sigma) for 5 to 30 min depending on mouse age. The cornea, lens, sclera, and vitreous were excised by limbal incision under a dissecting microscope. For flat mount preparation, retinas and choroids were detached and separated from the optic nerve with fine forceps. Radial incisions were made towards their edges. The flattened retinas were then washed with PBS and processed for β-gal activity assay and immunohistochemistry. For transverse section analyses, the retinas and choroids were not separated, instead they were immersed in 15% sucrose and OCT compound (TissUE-Tek) before being frozen in liquid N2 and cryostat-sectioned at 20 μm. Immunohistochemistry was performed as described (Lopes et al., 2011).

Xgal staining
*Msx1^lacZ^* and *Msx2^lacZ^* genes expression was visualized by Xgal staining as described by (Houzelstein et al., 1997). After staining, tissues were post-fixed in 4% PFA for 1 h at room temperature, then washed 3 times in PBS before immunohistochemistry.

Immunohistochemistry
Retinas were permeabilised with PBS containing 0.2% Triton X-100 and 50 mM NH4Cl for 30 min. Tissues were washed 3 times in PBS then treated for 1 h with blocking buffer (1 mM MgCl2, 1 mM CaCl₂, 10% goat serum and 0.5% Tween-20 in PBS). The same blocking solution was used for incubation with primary antibodies overnight at 4℃ under gentle agitation. Primary antibodies are listed in Table 1. The retinas were washed four times for 5 min with 0.1% Tween-20 in PBS, incubated for 1 h with secondary antibodies diluted in blocking buffer. Secondary antibodies (Invitrogen) were Alexa Fluor 488 goat anti-mouse and goat anti-rabbit, Alexa Fluor 568 goat anti-rabbit, Alexa Fluor 647 goat anti-mouse, Alexa Fluor 635 goat anti-rabbit at 1/300 and Alexa Fluor 488 streptavidin at 1/1000. Retinas were washed again three times for 5 min with 0.1% Tween-20 in PBS, followed by incubation with 2.5 μg/ml of Hoechst 33342 (bisBenzimide trihydrochloride, Sigma) in PBS for 15 min to label nuclei. They were finally

Table 1. Primary antibodies used in this study.

Antibody	Source	Dilution
Monoclonal anti-mouse α-SMA Cy3-conjugated	Sigma	1/1000
Monoclonal mouse anti-calponin	Sigma	1/500
Monoclonal mouse anti-desmin	Dako	1/250
Rabbit polyconal anti- proteoglycan NG2	Chemicon	1/200
Monoclonal rat anti-mouse CD31	BD pharmingen	1/200
Biotinylated isolectin B4	Molecular Probes	1/1000
Rabbit polyclonal anti-laminin	Sigma	1/400
Rabbit polyclonal anti-Gfp	Invitrogen	1/500
Polyclonal rabbit anti-b-galactosidase	Cappel	1/1500

washed in PBS and two times in water and flat mounted with Dako mounting medium.

Microscopy of retinal and choroid whole-mounts
Whole-mount retinas were primarily observed under a Zeiss Axiophot fluorescence microscope, and a Zeiss Axioplan equipped with an Apotome, and analysed with the Axiovison software (Carl Zeiss, Jena, Germany). Co-localizations were performed with a confocal microscope Zeiss LSM 700 equipped with the Zen software (Carl Zeiss, Jena, Germany). All captured images were assembled using Adobe Photoshop or Adobe Illustrator (Adobe Systems, San Jose, CA, USA). For quantitative analyses, one-way ANOVA was used to compare independent experiments. Comparison between data groups was performed with the non-parametric Dunnett test.

Competing Interests
The authors declare no competing interests.

References
Anderson, B., Jr and McIntosh, H. D. (1967). Retinal circulation. *Annu. Rev. Med.* **18**, 15-26.
Andersson, M., Karlsson, L., Svensson, P. A., Ulfhammer, E., Ekman, M., Jernas, M., Carlsson, L. M. and Jern, S. (2005). Differential global gene expression response patterns of human endothelium exposed to shear stress and intraluminal pressure. *J. Vasc. Res.* **42**, 441-452.
Armulik, A., Genove, G. and Betsholtz, C. (2011). Pericytes: developmental, physiological, and pathological perspectives, problems, and promises. *Dev. Cell* **21**, 193-215.
Bach, A., Lallemand, Y., Nicola, M.-A., Ramos, C., Mathis, L., Maufras, M. and Robert, B. (2003). *Msx1* is required for dorsal diencephalon patterning. *Development* **130**, 4025-4036.
Baez, S. (1977). Microcirculation. *Annu. Rev. Physiol.* **39**, 391-415.
Bandopadhyay, R., Orte, C., Lawrenson, J. G., Reid, A. R., De Silva, S. and Allt, G. (2001). Contractile proteins in pericytes at the blood-brain and blood-retinal barriers. *J. Neurocytol.* **30**, 35-44.
Benedito, R., Roca, C., Sorensen, I., Adams, S., Gossler, A., Fruttiger, M. and Adams, R. H. (2009). The notch ligands Dll4 and Jagged1 have opposing effects on angiogenesis. *Cell* **137**, 1124-1135.
Benjamin, L. E., Hemo, I. and Keshet, E. (1998). A plasticity window for blood vessel remodelling is defined by pericyte coverage of the preformed endothelial network and is regulated by PDGF-B and VEGF. *Development* **125**, 1591-1598.
Bensoussan, V., Lallemand, Y., Moreau, J., Saint Clement, C., Langa, F. and Robert, B. (2008). Generation of an *Msx2*-GFP conditional null allele. *Genesis* **46**, 276-282.
Bentzer, P., Kongstad, L. and Grande, P. O. (2001). Capillary filtration coefficient is independent of number of perfused capillaries in cat skeletal muscle. *Am. J. Physiol. Heart Circ. Physiol.* **280**, H2697-H2706.
Boas, D. A., Jones, S. R., Devor, A., Huppert, T. J. and Dale, A. M. (2008). A vascular anatomical network model of the spatio-temporal response to brain activation. *NeuroImage* **40**, 1116-1129.

Boon, R. A. and Horrevoets, A. J. (2009). Key transcriptional regulators of the vasoprotective effects of shear stress. *Hämostaseologie* **29**, 39-40, 41-43.

Brown, A. S., Leamen, L., Cucevic, V. and Foster, F. S. (2005). Quantitation of hemodynamic function during developmental vascular regression in the mouse eye. *Invest. Ophthalmol. Vis. Sci.* **46**, 2231-2237.

Campochiaro, P. A. (2000). Retinal and choroidal neovascularization. *J. Cell. Physiol.* **184**, 301-310.

Cauli, B., Tong, X. K., Rancillac, A., Serluca, N., Lambolez, B., Rossier, J. and Hamel, E. (2004). Cortical GABA interneurons in neurovascular coupling: relays for subcortical vasoactive pathways. *J. Neurosci.* **24**, 8940-8949.

Chen, Y. H., Ishii, M., Sun, J., Sucov, H. M. and Maxson, R. E., Jr. (2007). *Msx1* and *Msx2* regulate survival of secondary heart field precursors and post-migratory proliferation of cardiac neural crest in the outflow tract. *Dev. Biol.* **308**, 421-437.

Diaz-Flores, L., Gutierrez, R., Madrid, J. F., Varela, H., Valladares, F., Acosta, E., Martin-Vasallo, P. and Diaz-Flores, L., Jr. (2009). Pericytes. Morphofunction, interactions and pathology in a quiescent and activated mesenchymal cell niche. *Histol. Histopathol.* **24**, 909-969.

Friedman, E., Smith, T. R. and Kuwabara, T. (1964). Retinal Microcirculation in Vivo. *Invest. Ophthalmol.* **3**, 217-226.

Fruttiger, M. (2002). Development of the mouse retinal vasculature: angiogenesis versus vasculogenesis. *Invest. Ophthalmol. Vis. Sci.* **43**, 522-527.

Fruttiger, M. (2007). Development of the retinal vasculature. *Angiogenesis* **10**, 77-88.

Fu, H., Ishii, M., Gu, Y. and Maxson, R. (2007). Conditional alleles of *Msx1* and *Msx2*. *Genesis* **45**, 477-481.

Ganesan, P., He, S. and Xu, H. (2010). Analysis of retinal circulation using an image-based network model of retinal vasculature. *Microvasc. Res.* **80**, 99-109.

Goupille, O., Saint Cloment, C., Lopes, M., Montarras, D. and Robert, B. (2008). *Msx1* and *Msx2* are expressed in sub-populations of vascular smooth muscle cells. *Dev. Dyn.* **237**, 2187-2194.

Gyllensten, L. J. and Hellstrom, B. E. (1954). Experimental approach to the pathogenesis of retrolental fibroplasia. I. Changes of the eye induced by exposure of newborn mice to concentrated oxygen. *Acta Paediatr. Suppl.* **43**, 131-148.

Henkind, P. and De Oliveira, L. F. (1968). Retinal arteriolar annuli. *Invest. Ophthalmol.* **7**, 584-591.

Hofmann, J. J. and Luisa Iruela-Arispe, M. (2007). Notch expression patterns in the retina: An eye on receptor-ligand distribution during angiogenesis. *Gene Expr. Patterns* **7**, 461-470.

Holtwick, R., Gotthardt, M., Skryabin, B., Steinmetz, M., Potthast, R., Zetsche, B., Hammer, R. E., Herz, J. and Kuhn, M. (2002). Smooth muscle-selective deletion of guanylyl cyclase-A prevents the acute but not chronic effects of ANP on blood pressure. *Proc. Natl. Acad. Sci. USA* **99**, 7142-7147.

Houzelstein, D., Cohen, A., Buckingham, M. E. and Robert, B. (1997). Insertional mutation of the mouse *Msx1* homeobox gene by an *nlacZ* reporter gene. *Mech. Dev.* **65**, 123-133.

Hughes, S. and Chan-Ling, T. (2004). Characterization of smooth muscle cell and pericyte differentiation in the rat retina in vivo. *Invest. Ophthalmol. Vis. Sci.* **45**, 2795-2806.

Hughes, S., Gardiner, T., Hu, P., Baxter, L., Rosinova, E. and Chan-Ling, T. (2006). Altered pericyte-endothelial relations in the rat retina during aging: implications for vessel stability. *Neurobiol. Aging* **27**, 1838-1847.

Ikebe, T., Shimada, T., Ina, K., Kitamura, H. and Nakatsuka, K. (2001). The three-dimensional architecture of retinal blood vessels in KK mice, with special reference to the smooth muscle cells and pericytes. *J. Electron Microsc. (Tokyo)* **50**, 125-132.

Ishii, M., Han, J., Yen, H. Y., Sucov, H. M., Chai, Y. and Maxson, R. E., Jr. (2005). Combined deficiencies of *Msx1* and *Msx2* cause impaired patterning and survival of the cranial neural crest. *Development* **132**, 4937-4950.

Jain, R. K. (2003). Molecular regulation of vessel maturation. *Nat. Med.* **9**, 685-693.

Kisanuki, Y. Y., Hammer, R. E., Miyazaki, J., Williams, S. C., Richardson, J. A. and Yanagisawa, M. (2001). Tie2-Cre transgenic mice: a new model for endothelial cell-lineage analysis in vivo. *Dev. Biol.* **230**, 230-242.

Lallemand, Y., Nicola, M. A., Ramos, C., Bach, A., Saint Cloment, C. and Robert, B. (2005). Analysis of *Msx1*; *Msx2* double mutants reveals multiple roles for Msx genes in limb development. *Development* **132**, 3003-3014.

Lallemand, Y., Bensoussan, V., Saint Cloment, C. and Robert, B. (2009). Msx genes are important apoptosis effectors downstream of the Shh/Gli3 pathway in the limb. *Dev. Biol.* **331**, 189-198.

Lopes, M., Goupille, O., Saint Cloment, C., Lallemand, Y., Cumano, A. and Robert, B. (2011). Msx genes define a population of mural cell precursors required for head blood vessel maturation. *Development* **138**, 3055-3066.

Magistretti, P. J. and Pellerin, L. (1999). Cellular mechanisms of brain energy metabolism and their relevance to functional brain imaging. *Philos. Trans. R. Soc. London Ser. B* **354**, 1155-1163.

Metea, M. R. and Newman, E. A. (2006). Glial cells dilate and constrict blood vessels: a mechanism of neurovascular coupling. *J. Neurosci.* **26**, 2862-2870.

Mitchell, D. E. and Gingras, G. (1998). Visual recovery after monocular deprivation is driven by absolute, rather than relative, visually evoked activity levels. *Curr. Biol.* **8**, R897.

Muzumdar, M. D., Tasic, B., Miyamichi, K., Li, L. and Luo, L. (2007). A global double-fluorescent Cre reporter mouse. *Genesis* **45**, 593-605.

Nehls, V. and Drenckhahn, D. (1991). Heterogeneity of microvascular pericytes for smooth muscle type alpha-actin. *J. Cell Biol.* **113**, 147-154.

Ni, C. W., Qiu, H. and Jo, H. (2010). MicroRNA-663 upregulated by oscillatory shear stress plays a role in inflammatory response of endothelial cells. *Am. J. Physiol. Heart Circ. Physiol.* **300**, H1762-H1769.

Orlidge, A. and D'Amore, P. A. (1987). Inhibition of capillary endothelial cell growth by pericytes and smooth muscle cells. *J. Cell Biol.* **105**, 1455-1462.

Ozerdem, U., Grako, K. A., Dahlin-Huppe, K., Monosov, E. and Stallcup, W. B. (2001). NG2 proteoglycan is expressed exclusively by mural cells during vascular morphogenesis. *Dev. Dyn.* **222**, 218-227.

Pannarale, L., Onori, P., Ripani, M. and Gaudio, E. (1996). Precapillary patterns and perivascular cells in the retinal microvasculature. A scanning electron microscope study. *J. Anat.* **188**, 693-703.

Peppiatt, C. M., Howarth, C., Mobbs, P. and Attwell, D. (2006). Bidirectional control of CNS capillary diameter by pericytes. *Nature* **443**, 700-704.

Porat, R. M., Grunewald, M., Globerman, A., Itin, A., Barshtein, G., Alhonen, L., Alitalo, K. and Keshet, E. (2004). Specific induction of tie1 promoter by disturbed flow in atherosclerosis-prone vascular niches and flow-obstructing pathologies. *Circ. Res.* **94**, 394-401.

Rucker, H. K., Wynder, H. J. and Thomas, W. E. (2000). Cellular mechanisms of CNS pericytes. *Brain Res. Bull.* **51**, 363-369.

Saint-Geniez, M. and D'Amore, P. A. (2004). Development and pathology of the hyaloid, choroidal and retinal vasculature. *Int. J. Dev. Biol.* **48**, 1045-1058.

Sato, Y. and Rifkin, D. B. (1989). Inhibition of endothelial cell movement by pericytes and smooth muscle cells: activation of a latent transforming growth factor-beta 1-like molecule by plasmin during co-culture. *J. Cell Biol.* **109**, 309-315.

Satokata, I., Ma, L., Ohshima, H., Bei, M., Woo, I., Nishizawa, K., Maeda, T., Takano, Y., Uchiyama, M., Heaney, S. et al. (2000). *Msx2* deficiency in mice causes pleiotropic defects in bone growth and ectodermal organ formation. *Nat. Genet.* **24**, 391-395.

Shepro, D. and Morel, N. M. (1993). Pericyte physiology. *FASEB J.* **7**, 1031-1038.

Simoens, P., De Schaepdrijver, L. and Lauwers, H. (1992). Morphologic and clinical study of the retinal circulation in the miniature pig. A: Morphology of the retinal microvasculature. *Exp. Eye Res.* **54**, 965-973.

Srienc, A. I., Kurth-Nelson, Z. L. and Newman, E. A. (2010). Imaging retinal blood flow with laser speckle flowmetry. *Front Neuroenergetics* **2**, pii: 128.

Stahl, A., Connor, K. M., Sapieha, P., Chen, J., Dennison, R. J., Krah, N. M., Seaward, M. R., Willett, K. L., Aderman, C. M., Guerin, K. I. et al. (2010). The mouse retina as an angiogenesis model. *Invest. Ophthalmol. Vis. Sci.* **51**, 2813-2826.

Sweet, D. T., Chen, Z., Wiley, D. M., Bautch, V. L. and Tzima, E. (2011). The adaptor protein Shc integrates growth factor and ECM signaling during postnatal angiogenesis. *Blood* [Epub ahead of print] doi: 10.1182/blood-2011-10-384560.

Towler, D. A., Shao, J. S., Cheng, S. L., Pingsterhaus, J. M. and Loewy, A. P. (2006). Osteogenic regulation of vascular calcification. *Ann. New York Acad. Sci.* **1068**, 327-333.

Van Gieson, E. J., Murfee, W. L., Skalak, T. C. and Price, R. J. (2003). Enhanced smooth muscle cell coverage of microvessels exposed to increased hemodynamic stresses in vivo. *Circ. Res.* **92**, 929-936.

Weskamp, G., Mendelson, K., Swendeman, S., Le Gall, S., Ma, Y., Lyman, S., Hinoki, A., Eguchi, S., Guaiquil, V., Horiuchi, K. et al. (2010). Pathological neovascularization is reduced by inactivation of ADAM17 in endothelial cells but not in pericytes. *Circ. Res.* **106**, 932-940.

Wiedeman, M. P., Tuma, R. F. and Mayrovitz, H. N. (1976). Defining the precapillary sphincter. *Microvasc. Res.* **12**, 71-75.

Wu, L. Y., Li, M., Hinton, D. R., Guo, L., Jiang, S., Wang, J. T., Zeng, A., Xie, J. B., Snead, M., Shuler, C. et al. (2003). Microphthalmia resulting from *MSX2*-induced apoptosis in the optic vesicle. *Invest. Ophthalmol. Vis. Sci.* **44**, 2404-2412.

Xue, Y., Gao, X., Lindsell, C. E., Norton, C. R., Chang, B., Hicks, C., Gendron-Maguire, M., Rand, E. B., Weinmaster, G., Gridley, T. et al. (1999). Embryonic lethality and vascular defects in mice lacking the Notch ligand Jagged1. *Hum. Mol. Genet.* **8**, 723-730.

Ye, X., Wang, Y., Cahill, H., Yu, M., Badea, T. C., Smallwood, P. M., Peachey, N. S. and Nathans, J. (2009). Norrin, frizzled-4, and Lrp5 signaling in endothelial cells controls a genetic program for retinal vascularization. *Cell* **139**, 285-298.

Zarins, C. K., Giddens, D. P., Bharadvaj, B. K., Sottiurai, V. S., Mabon, R. F. and Glagov, S. (1983). Carotid bifurcation atherosclerosis. Quantitative correlation of plaque localization with flow velocity profiles and wall shear stress. *Circ. Res.* **53**, 502-514.

Zonta, M., Angulo, M. C., Gobbo, S., Rosengarten, B., Hossmann, K. A., Pozzan, T. and Carmignoto, G. (2003). Neuron-to-astrocyte signaling is central to the dynamic control of brain microcirculation. *Nat. Neurosci.* **6**, 43-50.